

## Non-Linear Analysis Spur Gear Mesh by Finite Element Method

التحليل اللاخطي لتعشيق ترس عدل باستخدام طريقة العناصر المحددة

M.sc. Ali Hammoudi. AL-Wazir / Mechanical Department / Kerbala Institute

M.sc. Amal A. Abdullah / Mechanical Department / Al-shatra Institute

### Abstract:

Gearing is one of the most critical components in mechanical power transmission systems ,the characteristics of an involute gear system including contact stresses, bending stresses, and the transmission errors (T.E.) for a given was performed on spur gear set.. Transmission error is considered to be one of the main contributors to noise and vibration in a gear set. Transmission error measurement has become popular as an area of research on gears and is possible method for quality control. To estimate transmission error in a gear system, the characteristics of involute spur gears were analyzed by using the finite element method. The contact stresses were examined using 2-D FEM models in ANSYS<sup>®</sup> ver (8). The results indicate that combined torsional mesh stiffness increases at double pair of teeth and decreased in single pair teeth due to mesh cycle and the change in torsional mesh stiffness leads to change in transmission error that causes noise and vibration.

### الخلاصة :

تتميز صناديق التروس الحديثة والتي تستخدم التروس ( المسننات ) بكونها تعمل بسرور عالية وتعرض إلى أحمال ديناميكية كبيرة , وعليه فإن التحليل الدقيق للأجهادات والتشوهات و الضوضاء المتولدة في الأسنان أمر ضروري لابد منه. تم إجراء دراسة عددية باستخدام طريقة العناصر المحددة باختبار عنصر ذو الثمانية عقد لإيجاد الأجهادات و التشوهات الناتج من خطأ النقل الأسناتيكي. تم التعرف على جزء من المصادر المسببة للضوضاء و الاهتزازات أثناء دوران التروس خلال دورة تعشيق كاملة والمتمثلة بجساءة تعشيق اللي و خطأ النقل الأسناتيكي عن طريق أعاقلة أحد التروس عن الحركة بينما يدور الترس الآخر ويتم تسليط أحمال مختلفة خلال دورة تعشيق كاملة. أتضح من النتائج انه خلال تحليل ترسين في حالة تماس زيادة جساءة تعشيق اللي في حالة تماس زوجين من الأسنان وتقل زيادة جساءة تعشيق اللي في حالة تماس زوج واحد من الأسنان ويؤدي ذلك إلى زيادة خطأ النقل الأسناتيكي المسبب للضوضاء والاهتزازات.

### NOMENCLATURES:

Symbol	Description
E	modulus of elasticity (N/m <sup>2</sup> )
F	Normal applied force (N)
F <sub>x</sub>	Load component in x- direction (N)
F <sub>y</sub>	Load component in y- direction (N)
K <sub>g</sub>	Individual tensional Stiffness of the Gear
K <sub>m</sub>	Combined tensional mesh stiffness
K <sub>p</sub>	Individual tensional Stiffness of the pinion
m <sub>o</sub>	Module (mm)
N	Number of teeth on gear wheel
R <sub>i</sub>	The pinion and gear pitch radius
R <sub>p</sub>	Radius of pitch circle (mm)
SMX	The maximum von Misses stress
TE	Static Transmission error
ν <sub>i</sub>	Poisson's ratio for gear i
σ <sub>H</sub> □	The maximum Hertz stress

$\sigma_{lmax}(S_{lmax})$       **The maximum (principle) tensile stress**

## Introduction

In the mechanics of solids and its engineering applications, contact effects are rarely seriously taken into account in conventional engineering analysis, because of the extreme. Complexity involved. Mechanical problems involving contacts are inherently nonlinear. The investigation of numerical methods for modeling the mechanism properties of involutes spur gear in mesh, over the mesh cycle, using the finite element method with 8-node isoparametric element, birth and death type element in ANSYS<sup>®</sup> forms the major part of this paper. The prime source of vibration and noise in a gear system is the transmission error between meshing gears. Transmission error is a term used to describe or is defined as the differences between the theoretical and actual positions between a pinion (driving gear) and a driven gear. It has been recognized as a main source for mesh frequency excited noise and vibration. With prior knowledge of the operating conditions of the gear set, it is possible to design the gears such that the vibration and noise are minimized [1]. To enable the investigation of contact problems with FEM, the stiffness relationship between the two contacts areas are usually established through a spring placed between the two contacting areas. This can be achieved by inserting a contact element placed in between the two areas where contact occurs. The literature available on the contact stress problems is extensive. But that available on the gear tooth contact stress problem is small, especially for transmission error including the contact problem. Klenz [2] examined the spur gear contact and bending stresses using two dimensional FEM. Coy and Chao [3] studied the effect of the finite element grid size on Hertzian deflection in order to obtain the optimum aspect ratio at the loading point for the finite element grid. Gatcombe and Prowell [4] studied the Hertzian contact stresses and duration of contact for a very specific case, namely a particular rocket motor gear tooth. Tsay [5] has studied the bending and contact stresses in helical gears using the finite element method with the tooth contact analysis technique. However, the details of the techniques used to evaluate the transmission error including contact stresses were not present.

## Case Illustrations

Table (1) shows the specifications of the gears used in this paper

Gear type -----	standard involute, full –depth teeth
Material -----	Steel
-----	Modulus of elasticity, $E \left( \text{N/m}^2 \right) 207 \times 10^9$
Passion's ratio, $v$ -----	0.3
Number of teeth, $N$ -----	24
Pressure angle, $\phi$ (deg)-----	20
Module, $m_o$ (mm)-----	12
Addendum, $a$ (mm)-----	$m_o$
Dedendum, $b$ (mm) -----	$1.157 m_o$
Theoretical contact ratio -----	1
Yield stress $\sigma_y$ , $(\text{N/m}^2)$ -----	$650 \times 10^6$
Ultimate stress $\sigma_u$ , $(\text{N/m}^2)$ -----	$900 \times 10^6$
Material density, $\rho$ $(\text{kg/m}^3)$ -----	7860
Power, $P$ (KW)-----	1500-1800
Angular Velocity, $\omega$ (rad/Sec)-----	78.5
Radius of pitch circle $R_p$ (m).....	0.144

### **Loading angle**

$$\text{Torque} = \frac{\text{Power}}{\text{Angular Velocity}} = (20 - 25) \text{KNm}$$

$$\text{Load} = \frac{\text{Torque}}{R_p} = \frac{25000 \text{Nm}}{0.144 \text{m}} \approx 175000 \text{N}$$

### **Gear tooth geometry**

A computer program is used APDL (ANSYS Parametric Design Language), so that the “one window” CAD/FED method could be applied to avoid the possible geometry data loss. In this program the graphic for any given gear is created. Since the program can draw gears quickly and easily, with a click of the mouse the shape of the tooth or gear is calculated to an accuracy of  $1 \times 10^{-4}$  mm and the area is plotted ,gear auto suitable mesh and boundary condition are integrated into one program in ANSYS [6]. In addition to plot of symmetrical and unsymmetrical single gear tooth ,a pair of teeth , two pairs of teeth engagement are also plotted as shown in Fig.(1).

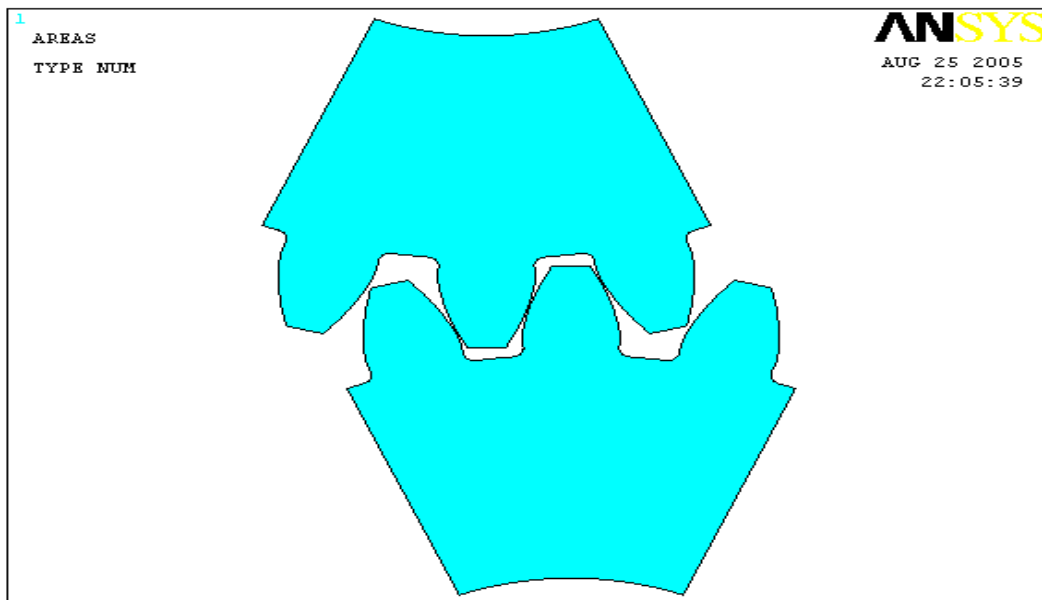


**Fig. (1) Gear tooth geometry**

### **Results and Discussions**

#### **The Use of Specified Coordinate system**

When the need arises for imposing loads or displacement boundary conditions in a direction that is not aligned with the global coordinate system, a specified coordinate system, local coordinate system, or working plane, may be defined at a desired location. The nodal coordinate system, which by default is parallel to the global Cartesian coordinate system in ANSYS<sup>®</sup>, of select node(s) can be rotated into the specified coordinate system. The other way to rotate nodal coordinate system is by using known rotation angles or direction cosine component values of the degree of freedom, forces, master DOF, coupled nodes, and constraint equations.

As shown in Fig. (2), the nodal coordinate system of the nodes on the hub was rotated into the working plane, defined as cylindrical, which has been moved to the centre of the hub. The applied boundary condition ( $W_{X_i} = 0$  or  $r_i = 0$ ) constrain the gear hub radially, allowing only free rotation. The restrained nodes also couple with the master node, which means that any constrained nodes would have the same value on  $W_Y$  (or  $\square$ ) if there were deformation or rigid body motion of the

gear. Input torque can be expressed as the sum of the applied nodal forces at radius  $r$ , where  $T$  is input torque load,  $n$  is the total number of constrained nodes,  $F_i$  is the tangential nodal force (usually  $F_i = F_o$ ),  $F_o$  is constant value) and radius  $r$  is the hub radius.

$$T = \sum_{i=1}^n F_i r \quad \text{-----} 1$$

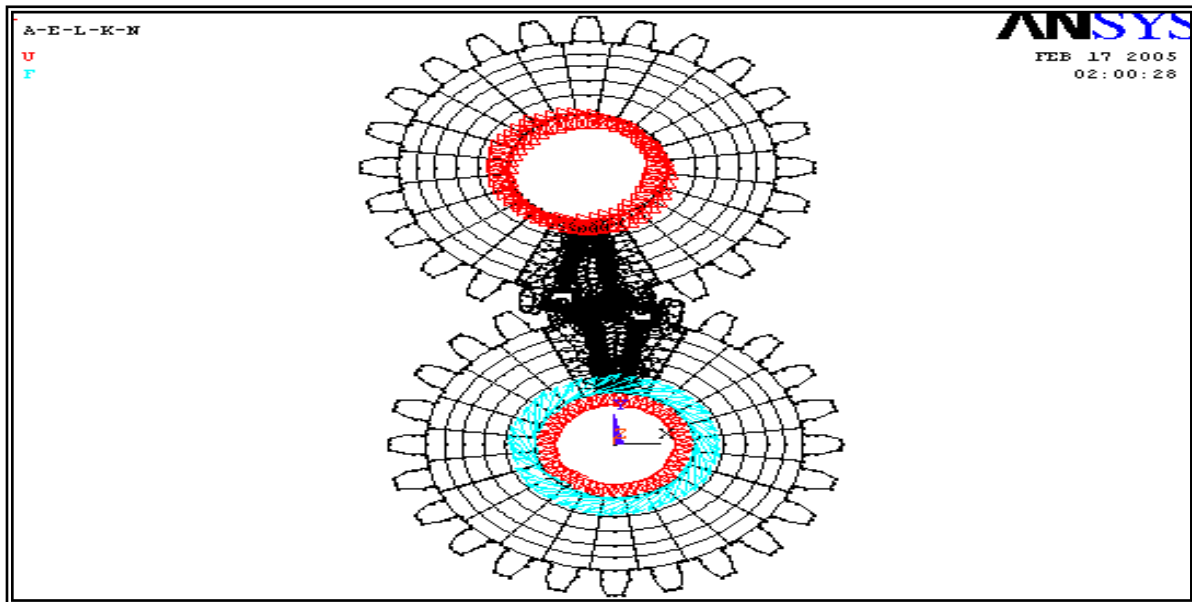


**Fig. (2) Loads, boundary conditions and coupling and reaction forces of the 2D plane stress.**

### Finite element mesh

Table (2) shows the results from an inertial coarse mesh, which has only (1665 ) nodes with the refinement gradually increasing the mesh density until the final model (model-10) has reached (17466 ) nodes. The displacement and stress values with their positions for each refinement are listed. Note that  $\sigma_{1\max}$  reaches the highest value close to the largest displacement value, however, the  $\sigma_{1\max}$  jumps to the position near the contact area with the increasing mesh density at the contact tooth, expect when some extra refinement was applied to tooth root at (model-8) and(model-10). Further calculations were carried out with model (6), with refinements applied to the area of the tooth root and the hub. There were two reasons for the further calculations.

- To verify the position of  $\sigma_{1\max}$ .
- To check the other influence (other than contact) on the displacement convergence.

The result in Table (3) shows that a refinement on the tooth root (the main part) and the hub is necessary for the determination of the convergence of  $\sigma_{1\max}$ , but the relative influence on the displacement convergence is minor.

The primary requirement for building FEA models of meshing pairs has been obtained from these results. Fig. (3) shows the studied case used in the research for obtaining reliable converged displacement values, while Table (4) shows the data mapped mesh of the studied case.

**Table (2) FEM calculation results**

Free mesh refine at contact point	Nodes No.	UY=(□*R) mm×10 <sup>-3</sup>	SMX contact at (Mpa)	σ <sub>1max</sub> (Mpa)	σ <sub>1max</sub> position
Model-1	1665	3.02484	52.41	24.32	near root
Model-2	1792	3.1957	65.23	26.83	near root
Model-3	2238	3.2435	71.98	49.862	near contact
Model-4	3393	3.3845	92.412	36.21	near contact
Model-5	4035	3.402	111.36	34.47	near contact
Model-6	5442	3.411	96.74	45.85	near contact
Model-7	6385	3.652	124.79	49.741	near contact
Model-8	8710	3.451	148.69	30.32	near root
Model-9	12755	3.417	183.319	31.25	near contact
Model-10	17466	3.502	221.36	30.51	near root

**Table (3) FEA results of further refinement for specify σ<sub>1max</sub> position**

Free mesh refine at contact point	Nodes No.	UY=(□*R) mm×10 <sup>-3</sup>	SMX contact at (Mpa)	σ <sub>1max</sub> (Mpa)	σ <sub>1max</sub> position
<b>Model-6</b>	5442	3.411	96.74	45.85	near contact
<b>Model6-1</b>	6049	3.458	105.64	44.231	near root
<b>Model6-2</b>	6408	3.4951	104.32	44.311	near root
<b>Model6-3</b>	6563	3.50145	106.84	44.254	near root

**Table (4) The data mapped mesh of the studied case.**

Mapped mesh	Nodes No.	UY=(□*R) mm×10 <sup>-3</sup>	SMX contact at (Mpa)	σ <sub>1max</sub> at toothroot (Mpa)
2D-183 plane stress	6563	3.50145	183.319	30.145

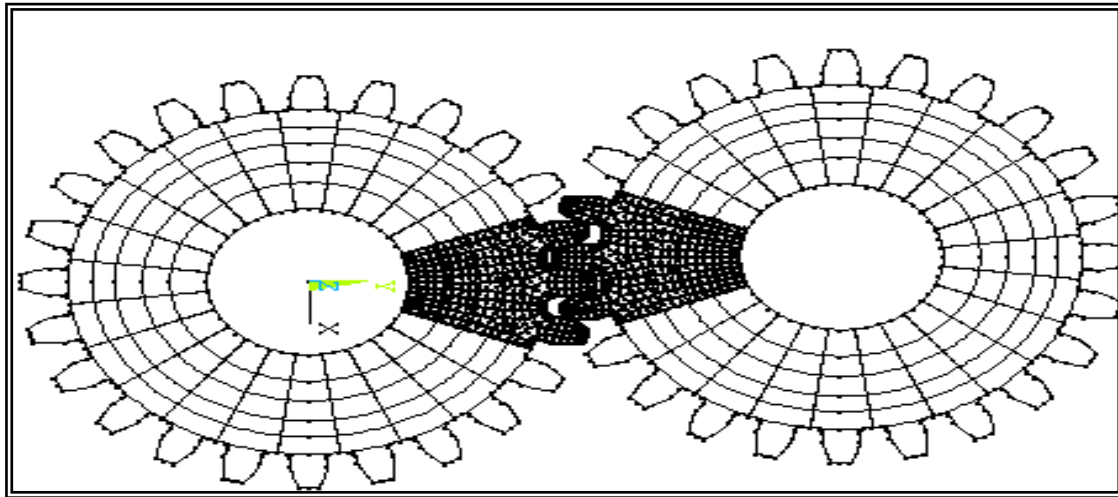


**Fig. (3) Finite Element Model of a meshing gear pair.**

The maximum surface (Hertz) stress [7]:

$$P_{\max} = \sigma_H = 0.564 \sqrt{\frac{F \left( \frac{1}{R_1} + \frac{1}{R_2} \right)}{\frac{1 - \nu_1^2}{E_1} + \frac{1 - \nu_2^2}{E_2}}} \quad \text{----- (2)}$$

$$\text{SMX} = 0.57 \sigma_H \quad \text{----- (3)}$$

The objective of the contact stress analyses was to gain an understanding of the modeling and solution difficulties in contact problems and examine the contact stresses in the gears. In order to verify the FEM contact model procedure, contact between two cylinders was modeled.

The comparison of results from FEM and the Hertzian theoretical formula is shown good agreement in table(5). The normal contact stress along the contact surface from the ANSYS solution is shown in Fig. (5) .This figure shows the distributions of the contact stress along the contact area.

**Table (5) Verification test for Contact Stress Analysis**

Stress (Mpa)		Percentage Deviation
<b>Hertzian formula</b>	<b>Present Work</b>	
181.7207	183.319	1.5983

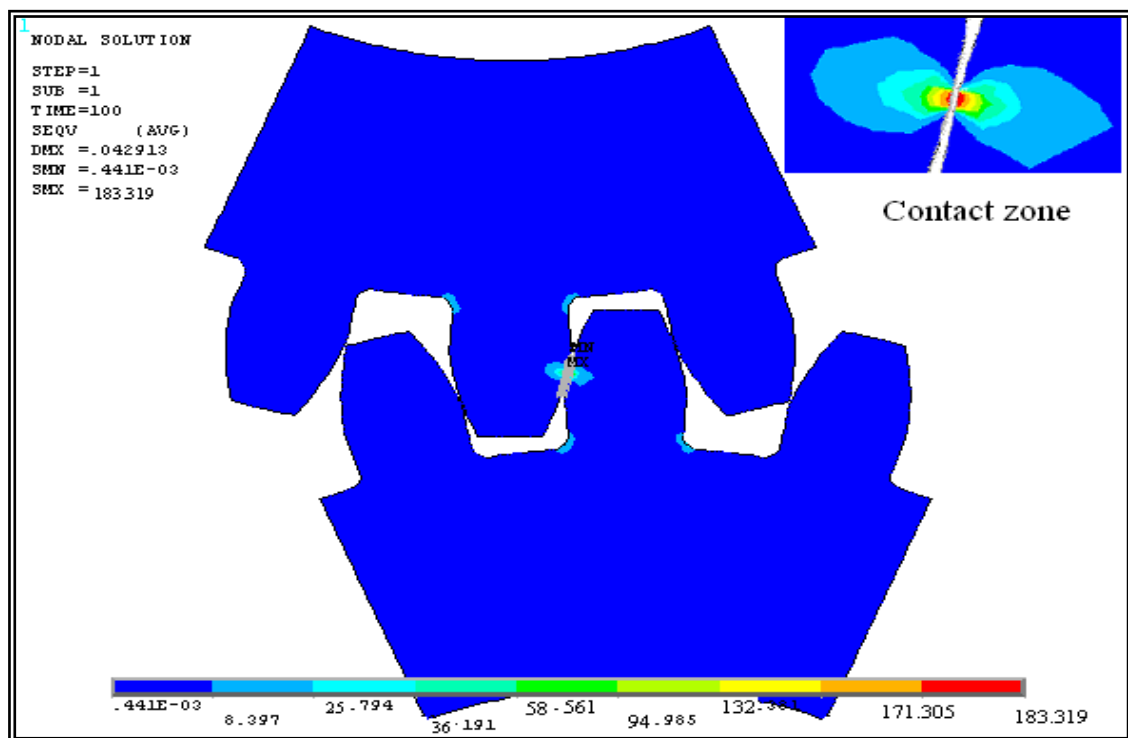


**Fig. (4) Normal contact stress along the contact surface.**

### **The Combined Torsional Mesh Stiffness**

One of many factors, which can be investigated, is the torsional mesh stiffness variation as the gear teeth rotate through the mesh cycle. With the current modeling capability, it is possible to predict the torsional mesh stiffness of two spur gears (multi-teeth) in mesh, where one of the gear hubs is restrained from rotating, with the other gear hub having a torque input load. The combined torsional mesh stiffness of two gears in mesh is calculated at each selected position in the mesh cycle, and the overall FEA solution shows that the combined torsional mesh stiffness varies with the meshing position as the teeth rotate within the mesh cycle. In particular, the combined torsional mesh stiffness decreases and increases dramatically as the meshing of the teeth changes from the double pair of teeth in contact, to the single pair of teeth in contact and vice-versa.

### **The Individual Torsional Stiffness**

In order to understand the combined torsional mesh stiffness, the variations of the individual torsional stiffness for each of the gears in the mesh cycle have to be studied. However, to predict the individual torsional stiffness for one of the gears in mesh is the rather complex procedure, due to the non-linear contact. The actual position of the contact(s) is usually unknown until the solution for both gears in mesh is completed.

A simple strategy for overcoming the difficulties can be developed, with a small torque input load, where one of the meshing gears can be modeled with rigid elements. In this case, the solutions for the combined torsional mesh stiffness in the mesh cycle are those given by the individual torsional mesh stiffness. When the input load is large, there certainly are errors in this strategy, and the relative error has to be estimated

### **The Individual Torsional Stiffness of the Pinion**

As shown in Fig. (5), the input torque load, boundary conditions and nodal couplings are applied on the drive gear (pinion) hub. Here, the plane stress assumption was used in the 2D modeling gears in mesh with flexible contact.

The ANSYS<sup>®</sup> eight node quad 183 series elements were chosen to produce a primary mapped mesh. Within a looping program, adaptive re-mesh with contact was used at each mesh position. It is possible to predict the individual torsional stiffness of the pinion of two spur gears (multi-teeth) in mesh, where the driven gear (gear) hubs is restrained from rotating, while the drive gear (pinion) hubs having a torque input load as shown in Fig. (5).

The first solution is calculated at the mesh position of the pitch point (0 degrees), then the pinion is rotated with an angle increment and the gear is rotated about O<sub>2</sub> for the next solution. There were

61 increments used here to cover the mesh cycle. In ANSYS<sup>®</sup>, the solution for angular displacement is given by tangential displacement value under the define polar coordinate system. Because the nodes on the drive gear hub were coupled with the master node in rotation, they will all have the same tangential displacement value UY as the master nodes, the Fig.(6) shows the tangential displacements on pinion hub under various loads. As given, the radius hub was r (mm). If  $\theta$  denotes the elastic angular rotation of the pinion hub, then

$$UY = r * \theta \quad \text{----- (4)}$$

So, the stiffness can be calculated by,

$$K_p = T / \theta = T * r / UY, \quad \text{----- (5)}$$

Where T is input torque load.

The major trend for the individual torsional stiffness over a complete is shown in Fig. (7). It can be seen that the hand over points from single to double teeth contact move slightly with increasing load, so that the single zone reduces when the input load increases, while, the double zone is relatively stable.

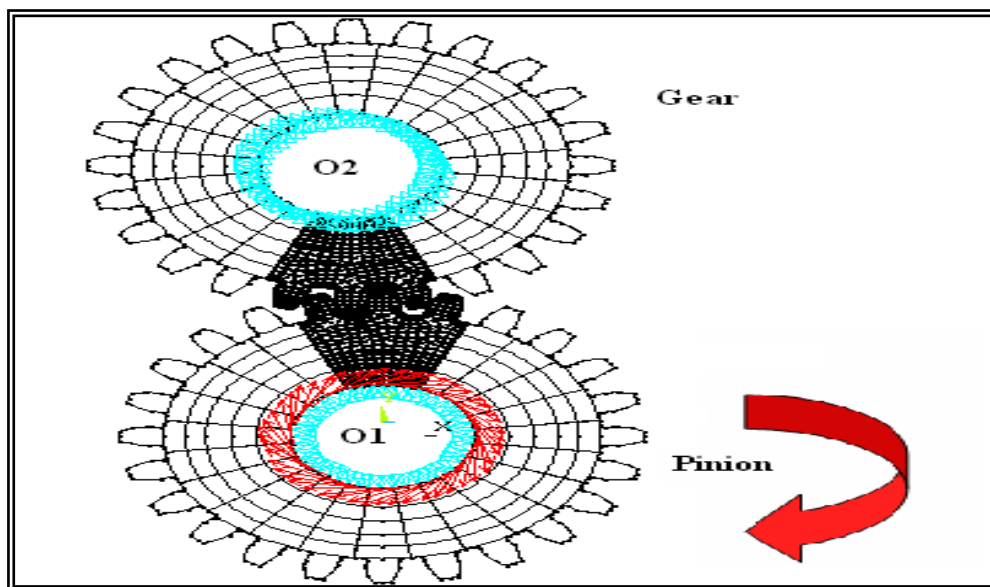


**Fig. (5)**

**The model for defining Individual Torsional Stiffness of the Pinion.**



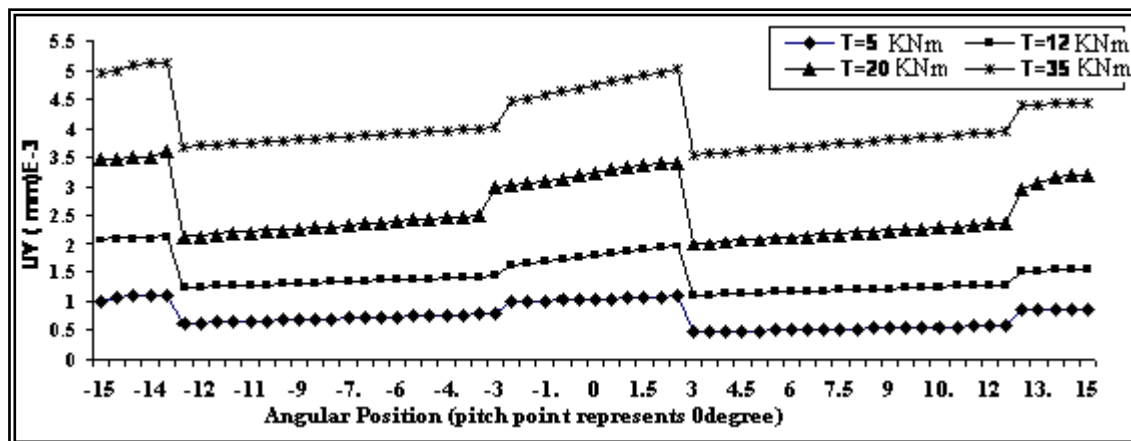


Fig. (6) Tangential displacements on pinion hub under various loads.

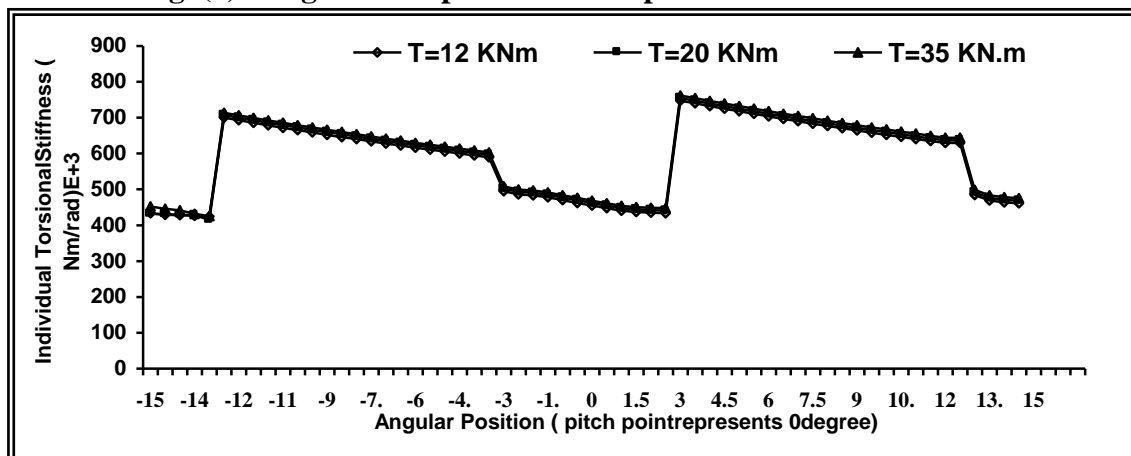


Fig. (7) The individual torsional stiffness on pinion hub under various loads.

### The Individual Torsional Stiffness of the Gear

As shown in Fig. (8), the input torque load, boundary conditions and nodal couplings are applied on the drive gear (pinion) hub. Here, the plane stress assumption was used in the 2D modeling gears in mesh with flexible contact.

The ANSYS<sup>®</sup> eight node quad 183 series elements were chosen to produce a primary mapped mesh. Within a looping program, adaptive re-mesh with contact was used at each mesh position. It is possible to predict the individual torsional stiffness of the gear of two spur gears (multi-teeth) in mesh, where the drive gear (pinion) hubs is restrained from rotating, while the driven gear (gear) hubs having a torque input load as shown in Fig. (8). The first solution is calculated at the mesh position of the pitch point (0 degrees), then the gear is rotated with an angle increment and the pinion is rotated about  $O_2$  for the next solution. There were 61 increments used here to cover the

mesh cycle. In ANSYS<sup>®</sup>, the solution for angular displacement is given by tangential displacement value under the define polar coordinate system. Because the nodes on the driven gear hub were coupled with the master node in rotation, they will all have the same tangential displacement value UY as the master nodes, the Fig. (9) shows the tangential displacements on gear hub under various loads. The major trend for the individual torsional stiffness over a complete is

shown in Fig. (10). It can be seen that the hand over points from single to double teeth contact move slightly with increasing load, so that the single zone reduces when the input load increases, while, the double zone is relatively stable.

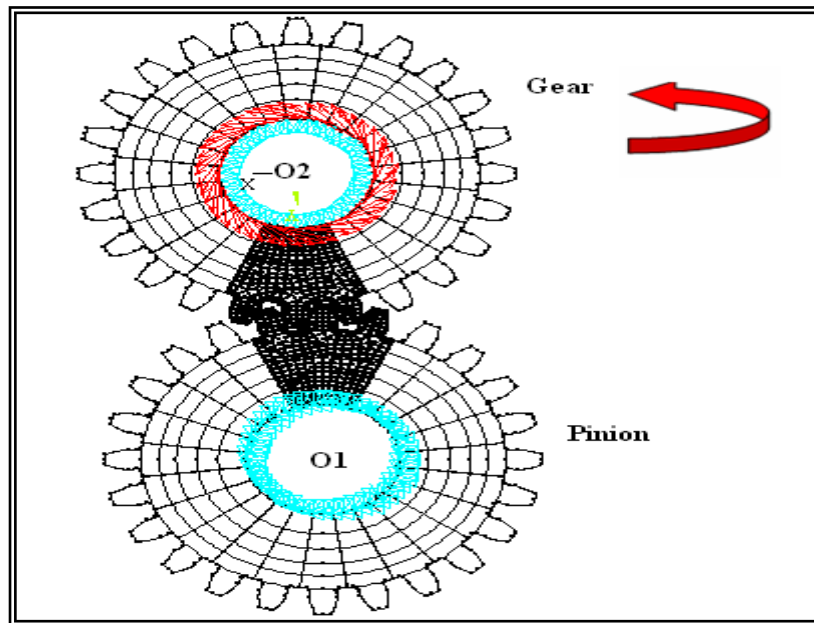


Fig. (8) The model for defining Individual Torsional Stiffness of the gear

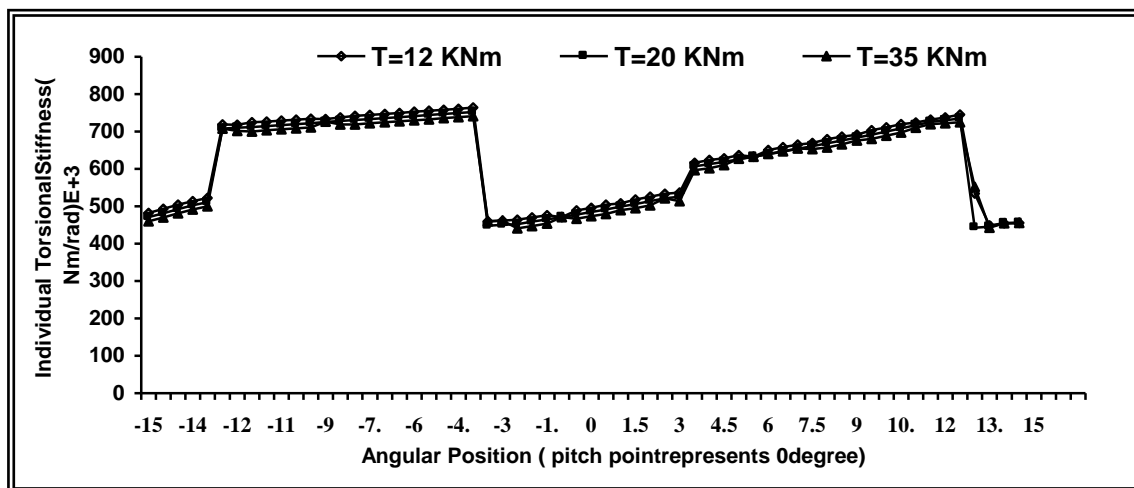


Fig. (9) Tangential displacements on gear hub under various loads

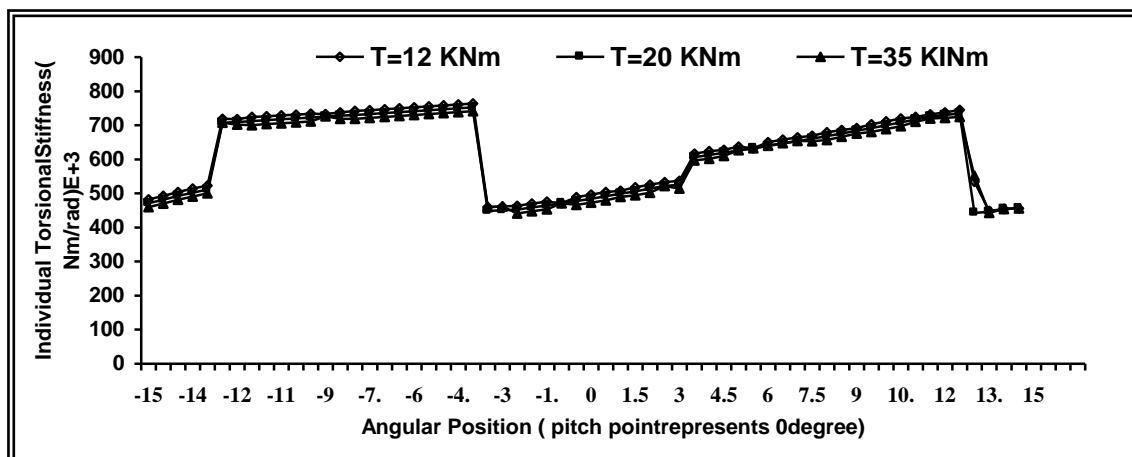


Fig. (10) The individual torsional stiffness on gear hub under various loads

### Discussions of the Combined Torsional Mesh Stiffness

The combined torsional mesh stiffness is derived from individual torsional mesh stiffness. At any position in the mesh cycle, gears can be modeled as two torsional springs connected in series. The system stiffness against input torque, so called the combined torsional mesh stiffness at each position, can be calculated by the following equation,

$$K_m = \frac{K_p * K_g}{K_p + K_g} \quad \text{----- (6)}$$

Where,  $K_p$  is the individual torsional mesh stiffness of the pinion,  $K_g$  is the individual torsional mesh stiffness of the gear and  $K_m$  denotes the combined torsional mesh stiffness.

Equation (6) can be used to calculate the results for the combined torsional mesh stiffness for different torque loads. Fig. (11) shows the combined torsional mesh stiffness results for a variation input load. From these results, the mesh position (angular position) varies over the complete mesh cycle. The dramatic change of the combined torsional mesh stiffness can be seen occur near the hand over points from single to double teeth in mesh and vice versa. The results tend to flat over the zone when the single pair of teeth in contact.

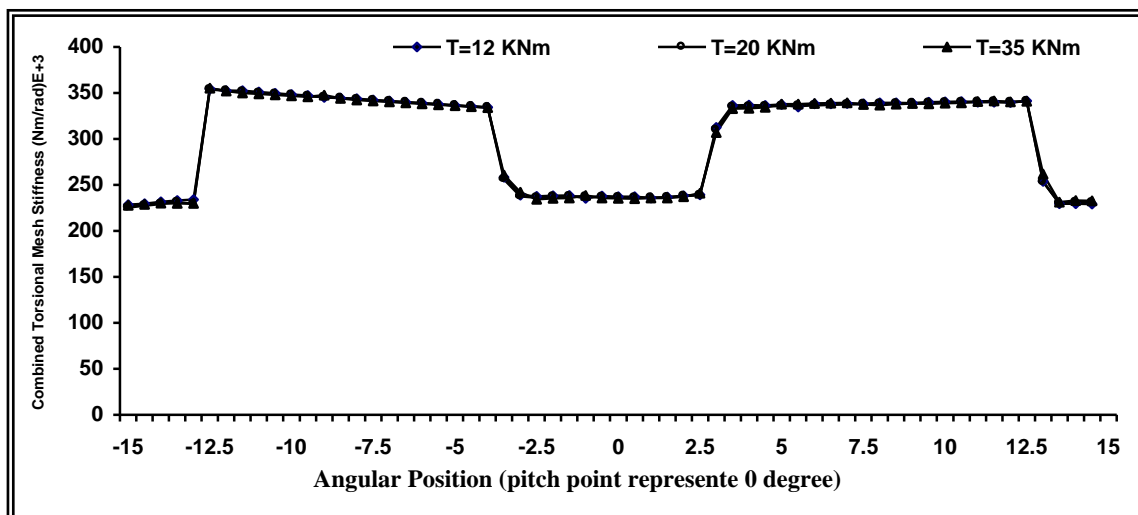


**Fig. (11) Combined Torsional Mesh Stiffness of mating gears over complete mesh cycle under various loads**

### Verification of the Combined Torsional Mesh Stiffness

In previous researches, the combined torsional mesh stiffness has been assumed to be constant at each mesh position, so that the combined torsional mesh stiffness was independent of the input torque load [8]. Using the adaptive re-mesh with contact, accurate results have been obtained as shown in Fig.(11), where it has been shown that the stiffness curve varies with the input torque load. In these solutions, except for the hand over points, the maximum stiffness difference in the (common) single and double zone is only about (0.01%). So, for most metallic gears in mesh, this difference might be ignored. It should be noted however, that the hand over points of the stiffness curves change their positions with various input torque loads. For the input torque variation from 12N.m to 35N.m, as given in Fig. (11), the results show nearly one degree of difference.

### The Static Transmission error

The term transmission error is used to describe the difference between the theoretical and actual input and output angular motions of gears in mesh. at low speed, the angular motions can be represented as angular positions of the input and output ends, so that the transmission error can be calculated by the following equation,

$$TE = \theta_g - (Z)\theta_p \quad \text{----- (7)}$$

where  $Z$  is the gear ratio and  $\theta_{g,p}$  denotes the angular rotation of the input and output gear in radians respectively.

### **The Static Transmission error for Perfect Involutes Gears in Mesh**

When gears are unloaded, a pinion and gear with involute profiles should theoretically run with zero transmission error. However, when gears with involutes profiles are loaded, the combined torsional mesh stiffness of the gears change, causing variations in angular rotation at the output gear hub or the shaft. At each particular meshing position, the angular rotation of the loaded drive gear due to tooth bending, shearing and contact displacement is calculated in the gear reference frame by restraining the driven gear from rotating. In relation to the drive gear reference frame, it is restrained from further rotating, while the torque input load and the resulting angular rotation of the gear is computed. The angular rotation is the static transmission error of gears under load at low speed, which can be expressed in angular units as shown in Eq. (7).

For perfect involute gear in mesh, with rigid mounting linear elastic material properties, the relationship between the input torque ( $T$ ) and the angular rotation of the gear hubs ( $\theta$ ) exists throughout every position of a mesh cycle as shown in equation below: -

$$T = K_m * \theta \quad \text{----- (8)}$$

Where  $K_m$  represents the combined torsional mesh stiffness and  $\theta$  represents the relative angular position difference between the hubs of the mating gears in mesh which is due to the pure elastic deformation.  $\theta$  remains zero only if the mating gears are perfectly rigid. Therefore, in a mesh cycle,  $\theta$  will denote the transmission error of the mating gears. In the 2D modeling of studied case, the transmission error can be shown in the Fig. (12).

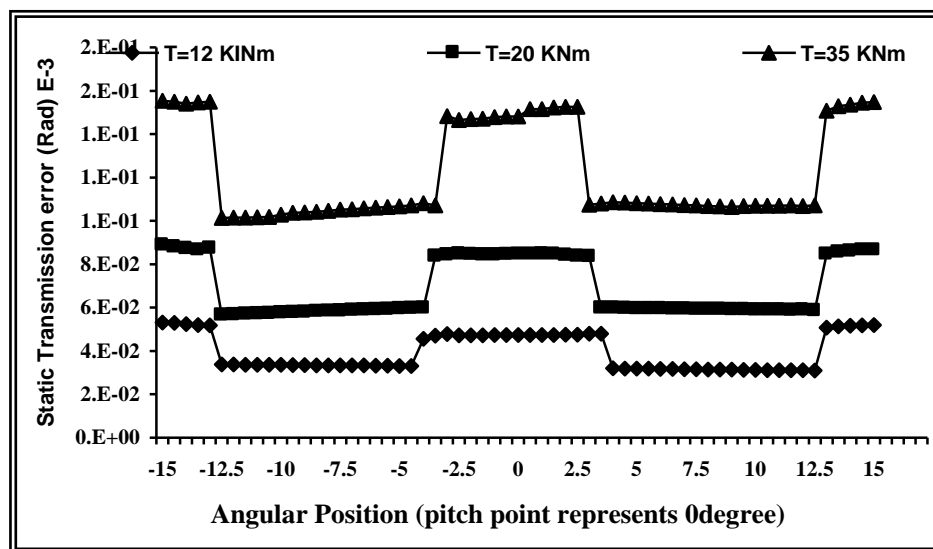


**Fig. (12) The transmission error of mating gears over complete mesh cycle under various loads**

### **Verification Test for the Static Transmission error**

The studied gear in Ref.[1] is a spur gear of module (3.75mm) , pressure angle ( $20^\circ$ ) , number of teeth (27) and speed ratio equal (1) . The material of the model is steel. Fig. (13) shows the comparison between the ANSYS<sup>®</sup> ver.(8) and Ref.[1], this comparison shows that there is a good

agreement between them, therefore the validity of the ANSYS<sup>®</sup> ver.(8) of calculate transmission error is satisfied.

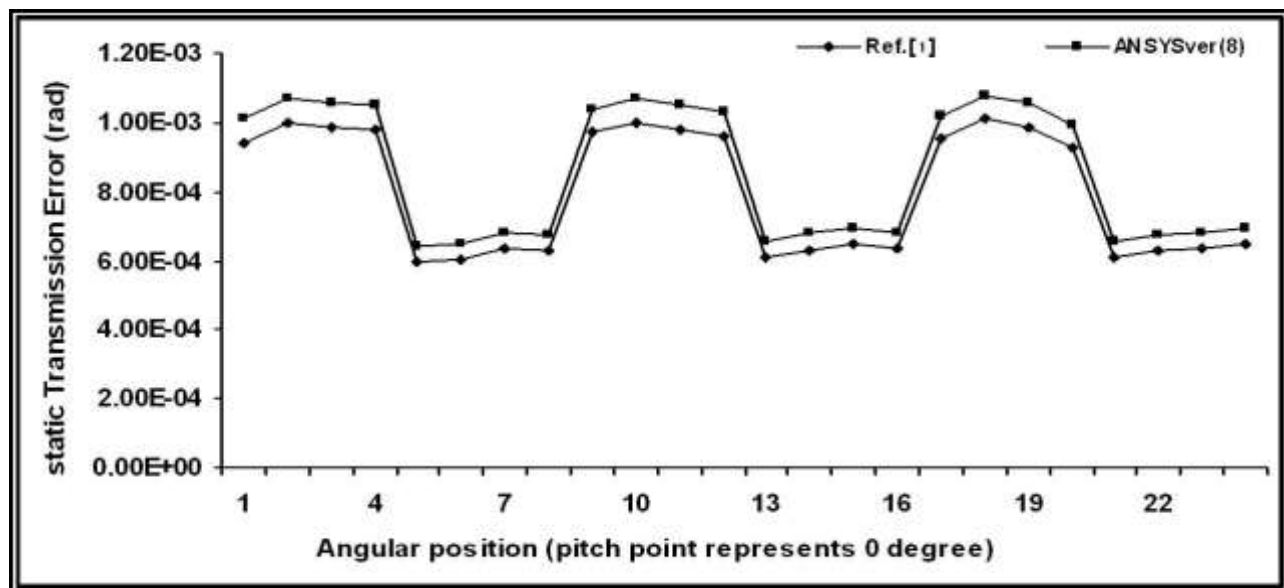


Fig. (13) Comparison between the Ref. [1] and ANSYS<sup>®</sup>,ver (8) for transmission error.

## Conclusions

- 1.The major thrust of this study has been the development of efficient and reliable numerical solution techniques using automatic mesh adaptation with the contact and the element birth and death option. This includes a fundamental study on the effect of plane stress. The numerical approach enabled the development of a software program based on the software package ANSYS<sup>®</sup> to predict the effect of the gears of torsional mesh stiffness, transmission error and ratio of local deformation.
- 2.The accuracy and the efficiency of the developed numerical models have provided the numerical results with more details of the change over process than previously obtained, and this was proved to be an important basic tool in the numerical analysis in gears in mesh.
3. The handover region of involute spur gears can include both the approach and recess cases, and it generally exists when gears are considered elastic. It is a key component of gear behavior that can be found in the combined torsional mesh stiffness, transmission error and ratio of local deformation and even in the individual torsional mesh stiffness characteristics. In particular, the handover region of the static T.E. represents the TE (in pervious research), the theory and evaluation method were developed mathematically (geometrical analysis), and they were found to be suitable for gears with geometrical errors.

**References:**

- [1] Parker, R. G., Vijayakar, S. M., and Imajo, t., “Non-Linear Dynamic Response of a Spur Gear Pair: Modeling and Experimental Comparisons,” Ohio State University, USA, Journal of Sound and Vibration, pp. 335-355, April 2000.
- [2] Klenz, S. R., “Finite Element Analyses of A Spur Gear Set”, M.Sc. Thesis ,Dept.of Mechanical Engineering, University of Saskatchewan, 1999.
- [3] Coy, J. J., Chao, C. H. S., “A method of selecting grid size to account for Hertz deformation in finite element analysis of spur gears ”, Trans. ASME , J.Mech. Design 104 759-766, 1982.
- [4] Gatcombe, E.K., Prowell , R.W., “ Rocket motor gear tooth analysis ”, (Hertzian contact stresses and times) Trans. ASME, J. Engng Industry, 1960.
- [5] Tsay, C.B., “Helical gears with involute shaped teeth: Geometry, computer simulation, tooth contact analysis , and stress analysis ” , Trans , J . Mechanisms,Transmissions, and Automation in Design , 1988
- [6] Amal A. Abullah,“ Analysis of a spur gear set by finite element method,”M.Sc. Thesis, Foundation of Technical Education, Technical College- Baghdad, 2005.
- [7] Hamrock, B. J., Jacobson, S. R., “Fundamentals of Machine Elements”.
- [8] Sirichai S., “ Torsional Properties of Spur Gear in Mesh using nonlinear Finite Element Analysis”, Ph.D. Thesis, Curtin University of Technology, 1999.